Reprinted from ENGINEERING FOR POWER, *Vol. 102, No. 4, October, 1980*

G. Fabris[1]
Mem. ASME

J. C. F. Chow[2]
P. F. Dunn

Engineering Division,
Argonne National Laboratory,
Argonne, IL 60439

On Formation of a Homogeneous Two-Phase Foam Flow[3]

This paper presents the results of a series of experiments conducted to evaluate the fluid mechanical performance of various two-phase LMMHD mixer designs. The results from both flow visualization studies of the local two-phase flows downstream from various mixer-element configurations and local measurements performed to characterize these flows are presented. A conceptual LMMHD mixer design is described that insures the generation of small bubbles, prevents the formation of gas slugs and separated regions, and favors the stabilization of a homogeneous foam flow.

Introduction

Although a mixer of gaseous and liquid phases is an important component in many current chemical and mechanical engineering systems, surprisingly little attention has been directed toward its proper design from a fluid-mechanical point of view. Some applications require a mixer to create a fine spray of liquid droplets in a gaseous medium, while others, as in the case of a LMMHD (liquid-metal magnetohydrodynamics) mixer, require a uniform dispersion of gaseous bubbles in a liquid medium.

Certain requirements for LMMHD mixer design result from the mixer's relation to the LMMHD energy conversion system. A schematic representation of the two-phase LMMHD system is shown in Fig. 1 and the typical LMMHD mixer-generator arrangement in Fig. 2. Refer to Fabris and Hantman [1] for a recent review on the specifics of the system. The heat-to-mechanical-to-electrical energy conversion characteristics of this LMMHD system require that the mixture's void fraction in the generator be high (on the order of 0.8 or greater) for maximum cycle efficiency (assuming generator isentropic efficiency is not significantly lowered with increasing void fraction.) This is achieved through the creation of a stable two-phase homogeneous foam flow of high void fraction by the mixer. Prediction codes developed at ANL have shown that if such a flow is maintained in the generator the isentropic efficiency of the LMMHD generator remains high provided the two-phase mixture behaves as a no-slip[4] homogeneous fluid.

It was proposed by Fabris, et al. [2] to use surface-active additives for liquid metals in order to prevent bubble coalescence, thereby creating a high-void-fraction foam flow with essentially zero slip. Such a foam flow behaves as a single-phase fluid with expansion properties very similar to that of a gas (important for heat-to-mechanical energy conversion). Literature on the formation of such a bubbly two-phase high-void fraction mixture is non-existent. However, some studies relevant to this problem have been made. Kling [3] experimentally investigated the injection of a gas through a single orifice into a stagnant liquid column at various pressure differentials and found a limiting bubble production rate. Wallis [4] showed that a surface-active liquid is a "necessary but not sufficient condition" for the creation of a homogeneous foam flow. These results indicate that increased surface activity delays the transition to slug flow with increasing void fraction, provided the air injection velocity remains below a critical superficial air velocity (Fig. 3). Further, if small superficial air injection velocities (<0.05 m/s) are maintained, high-void-fraction bubbly flows can be readily achieved. Staub [5] also pointed out that the manner of gas injection can have a detrimental influence on the resulting two-phase flow pattern and velocity slip between the gas and liquid phase when the liquid component is surface-active. Fujii-e, et al. [6] have noted that the increased turbulence intensity of the liquid at the entrance of a two-phase flow mixer strongly influences the resulting two-phase flow pattern and increases slip. Prins [7] made an attempt to derive a theoretical formulation on how velocity fluctuations in already generated foam flows could destroy it for some surface-active systems. More recently, Adler [1], testing two different air injection devices, revealed that the resulting non-surface-active high-void-fraction two-phase flow in both cases manifested practically the same flow characteristics.

All of the above clearly point out the importance of the proper design of a two-phase flow mixer which would create a homogeneous and stable foam of high void fraction at the entrance to a LMMHD generator. These considerations led to the initiation of the experiments described below.

Experimental Facility

A schematic of the ANL (Argonne National Laboratory) two-phase air-water test facility and its mixer design-evaluation test section is shown in Fig. 4. The 0.1 m × 0.1 m × 2.0 m vertically-aligned plexiglas test section utilizes a perforated plate at its domestic water supply inlet to create a uniform high level of downstream turbulence and a uniform velocity profile. A honeycomb made of packed straws then reduces the turbulence level perpendicular to the flow and provides a further uniform large obstruction, thereby producing a relatively-high pressure drop which reduces the streamwise component of turbulence. The flow downstream of the honeycomb is uniform with a low turbulence level. Further, the wall boundary layers are thin since

---

[1] Present affiliation: Senior Scientist, Combustion Dynamics and Propulsion Technology Division, Science Applications Inc., 21133 Victory Blvd., Canoga Park, CA. 91303.

[2] On sabbatical leave from the University of Illinois at Chicago Circle.

[3] Work prepared under the auspices of the U.S.D.O.E. and supported in part by the Office of Naval Research.

[4] Slip refers to the positive difference between the gas and liquid velocities at a particular cross section. It depends on the effectiveness of coupling between the liquid and gas phases and is inversely related to bubble coalescence.

Contributed by the Facilities Design Committee for publication in the JOURNAL OF ENGINEERING FOR POWER. Manuscript received at ASME Headquarters October 9, 1979.

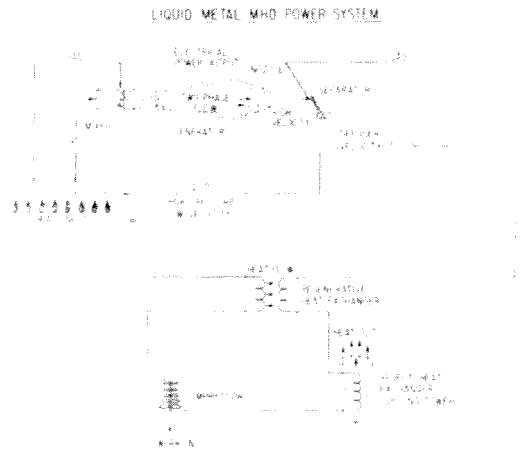

Fig. 1 Schematic of the LMMHD energy conversion system

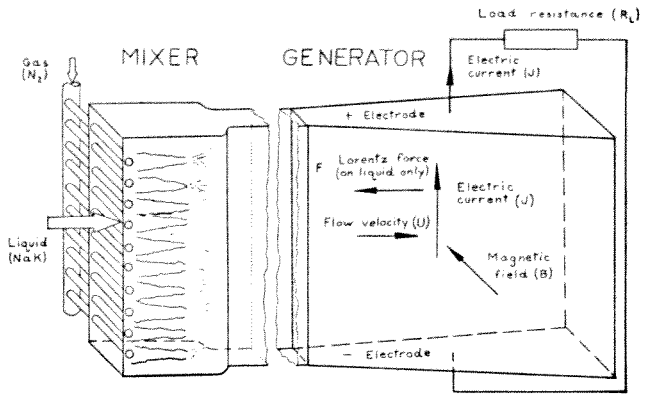

Fig. 2 Typical LMMHD mixer-generator configuration

they originate downstream of the honeycomb. Series of pressure taps and ports for the insertion of resistivity and hot-film probes are located along the test section length.

Compressed laboratory air is supplied via a manifold to the mixer elements. Both air and water flow meters are used to determine the inlet two-phase mixture quality. Various means of slow- and high-speed photography (Polaroid, 35mm, and Fastax cameras) are employed in conjunction with different ambient and stroboscopic lighting techniques to visualize the local two-phase flow.

The two-phase flow's local void fraction is measured via fine resistivity probes used in conjunction with resistivity probe and discriminator circuits developed for these experiments (Fig. 5). A gamma-ray attenuation system employing thullium sources is also present to obtain average void fraction profiles and these are compared with those obtained using the resistivity-probe method. Fig. 6 represents comparison of the average void fractions obtained by the resistivity probe and the γ-ray system. Agreement was reasonable even when a surfactive soap solution was used.

Plexiglas plates of different dimensions are inserted in the test section for each of the four mixer elements tested (single-tube, nine-tubes, nine-tubes with downstream contraction, and airfoil configurations). All tubes are 0.25 in. (0.6 cm) dia stainless steel tubing, with 0.076 in. (0.2 cm) size holes positioned 0.19 in. (0.5 cm) apart, staggered in two rows each 45 deg directed into the flow. The typical channel cross-sectional area of 1 × 4 in. (2.5 × 10 cm) is reduced to 0.5 × 4 in. (1 × 10 cm) at 2 in. (5 cm) downstream from the mixer elements for the case of the nine tubes with an abrupt downstream contraction.

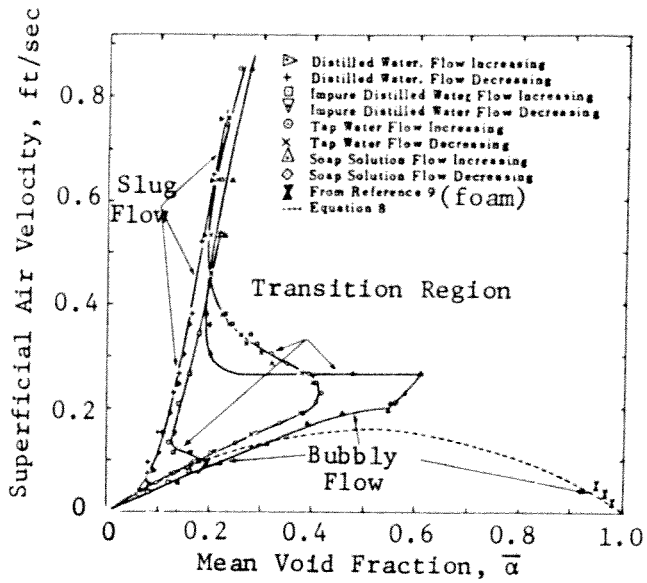

Fig. 3 Influence of surface activity on superficial air velocity in a bubbling column (Wallis, [4])

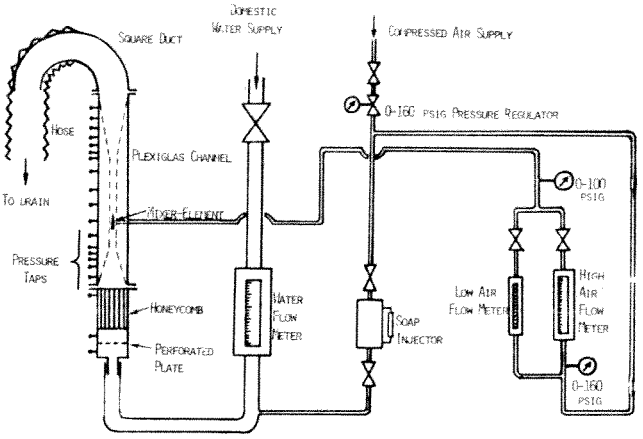

Fig. 4 Schematic of the air-water test facility

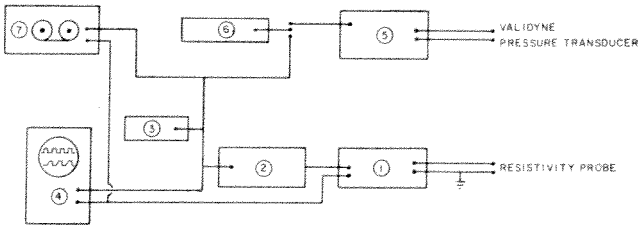

Fig. 5 Schematic of the data acquisition arrangement

Nomenclature

$\dot{V}_G$ = volumetric gas flow rate
$\dot{V}_L$ = volumetric liquid flow rate
U = axial velocity
α = local void fraction
$\bar{\alpha}$ = average void fraction of the cross-sectional area
$\beta = \dot{V}_G/(\dot{V}_G + \dot{V}_L)$

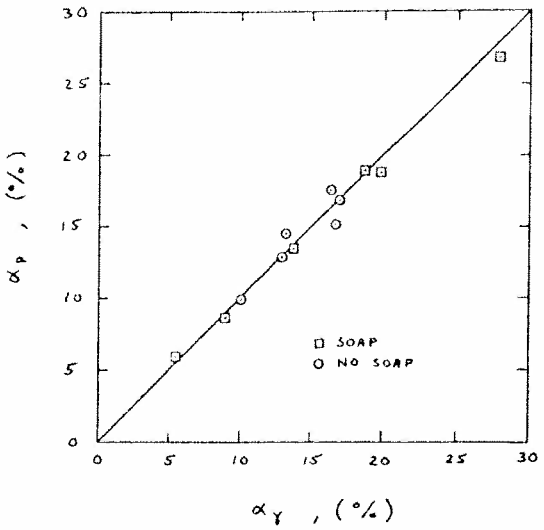

Fig. 6 Comparison of average void fractions obtained by the resistivity probe and a γ-ray system

Experimental Procedure

Each test run consisted of three different air flow rates at a predetermined constant water flow rate. For a given air flow, static pressures along the channel were measured in addition to local void fractions and bubble frequencies. Local void fractions were obtained approximately 12 in. (30 cm) downstream of the mixer element in both cross-sectional directions at a minimum of five cross-channel points. The bubble frequencies were recorded three times at each probe location for a duration of 10 s.

For flow visualization, 35 mm and Fastax cameras were used. The probe responses were observed on an oscilloscope and photographed using a Polaroid camera. In some selective runs, the probe responses were recorded on tape for further analysis. For a single-tube mixer, the void fractions were taken only along the narrow portion of the channel, but at two locations along the channel instead of one. In some instances, a soap solution (surfactant) was injected into the inlet water to determine the effect of increased surface activity.

Experimental Results

The typical operating parameter ranges included volumetric flow rates of water from 0.06 to 0.4 $\times 10^{-2}$ m^3/s and air from zero to 2.19 $\times 10^{-2}$ m^3/s, and local and averaged void fractions from zero to 0.8 and zero to 0.43, respectively. The results of tests for the various mixer designs are summarized in the following.

Single-Tube Mixer in a Straight Channel. The local void fraction and the bubble frequency were measured approximately 3 in. (8 cm) and 12 in. (30 cm) downstream of the mixer element to study the development of the mixing process in the channel. Measurements showed that near the mixer element the air was concentrated in the center portion of the channel, and further downstream the void-fraction distribution assumed a parabolic shape (see Fig. 7).

Experiments with soap solution injected upstream exhibited almost no noticeable change in void fraction profile shape and magnitude and in measured bubbling frequency. The slow injection of air in stagnant water produced bubbles of widely different sizes and shapes, as is evident in Fig. 8. Turbulent vortices created by the movement of large gas bubbles had the tendency to break the bubbles into smaller ones. Note that this "favorable effect" of turbulence exists only at low average void fractions (~0.1).

The high injection of air into stagnant water created churn turbulent slugs with water splashing up and down making observation in the region of gas injection difficult. When a lower water flow rate was applied, water would sweep exiting gas bubbles around the tube (due to the high momentum of the water with respect to the air) as shown in Fig. 9. A separated air-filled region was formed at the trailing edge of the mixer injection tube. The separated region broke up into bubbles of widely different sizes and shapes. This irregularity in shapes

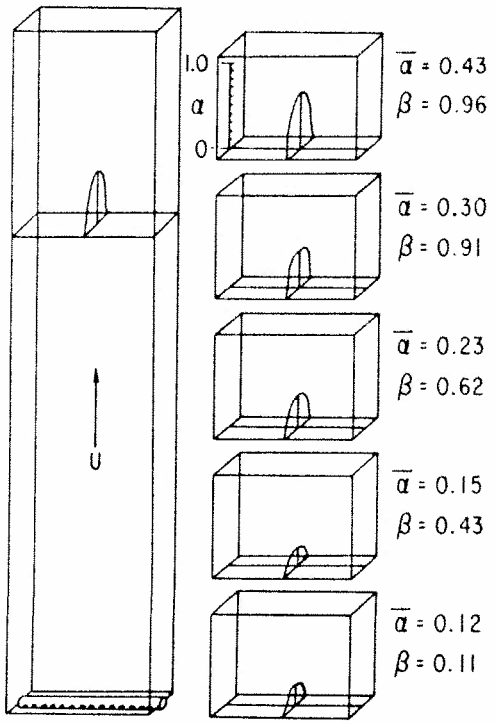

Fig. 7 Single-tube mixer in a straight channel: local void fraction profiles V_L = 0.06(*a*), 0.2(*b*), 0.06(*c*), 0.06(*d*), 0.4(*e*) $\times 10^{-2}$ m^3/s

Fig. 8 Two-phase flow pattern for a single-tube mixer in a straight channel: zero water flow rate and low air flow rate

was attributed to the influence of vortices and, to some degree, to coalescence. Increasing the velocity of the water resulted in more than a proportional increase in the length of the separated region. At high velocities the air-water interface appeared relatively flat with many small-scale waves.

Nine-Tube Mixer in a Straight Channel. The measurements were taken approximately 12 in. (30 cm) downstream from the tubes. (This distance is roughly the same as the length from the mixer to the generator entrance in the present ambient-temperature LMMHD generator experiment at ANL.) Two-phase flow patterns obtained are illustrated in Fig. 10. Distinct separated regions were found to form downstream of each tube. These individual separated regions persisted for several tube diameters downstream, and their length in-

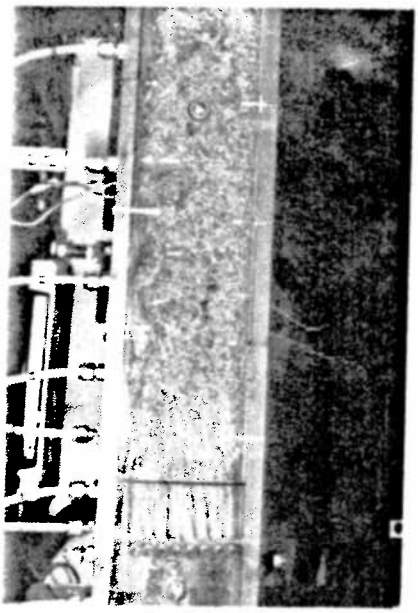

Fig. 9 Two-phase flow pattern for a single-tube mixer in a straight channel: medium water and medium air flow rates

Fig. 10 Two-phase flow pattern for a nine-tube mixer in a straight channel: medium water and medium air flow rates

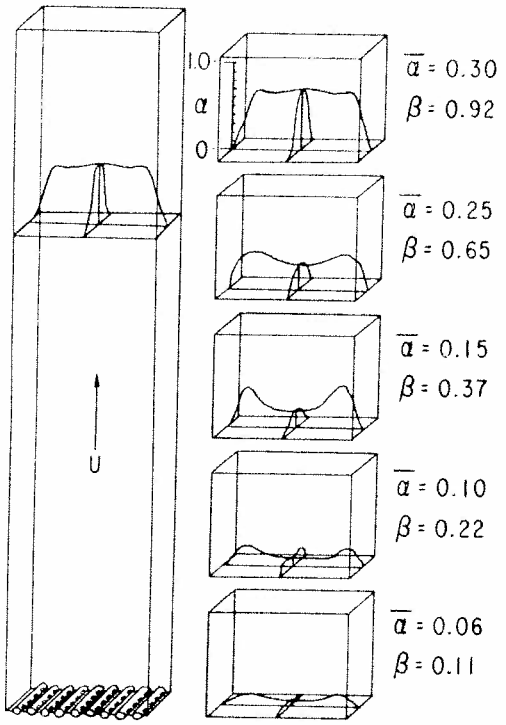

Fig. 11 Nine-tube mixer in a straight channel: local void fraction profiles V_L = 0.02(*a*), 0.06(*b*), 0.2(*c*), 0.2(*d*), 0.4(*e*) × 10^{-2} m^3/s

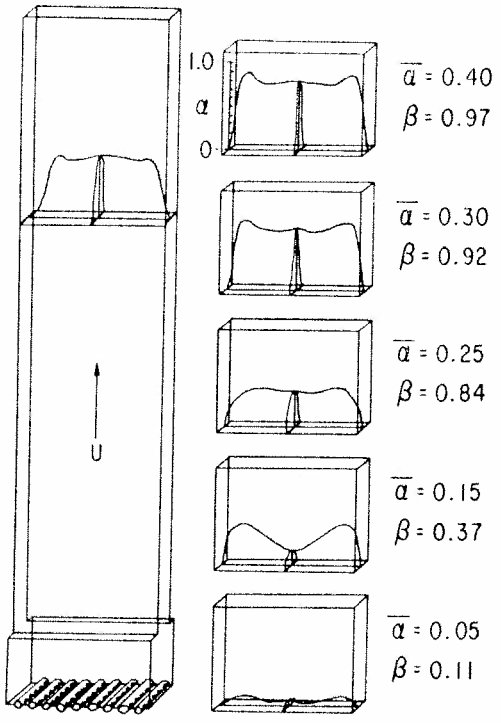

Fig. 12 Nine-tube mixer in a straight channel with an abrupt contraction: local void fraction profiles V_L = 0.06(*a*), 0.2(*b*), 0.4(*c*), 0.2(*d*), 0.4(*e*) × 10^{-2} m^3/s

creased with increasing water flow rate. Details of the mechanism of break-up of the separated regions were difficult to observe. Observations made along the narrower side of the channel revealed that a continuous air-water interface existed on the narrow side of the channel. Measurements showed that for a given water flow rate, the lateral void fraction distribution changed from a parabolic-like to a Gaussian-shaped distribution as the air flow rate increased. This was likely caused by a rapid migration of the bubbles toward the center of the channel due to bubble coalescence brought about by increased agitation. The void-fraction measurement made near the tubes showed a more-parabolic-like distribution. The depression of the void-fraction distribution in the central portion of the channel (see Fig. 11) across the wide cross-sectional area was probably caused by the higher stagnation pressure of the faster-moving water in the central portion. This induced a lower air flow rate for the perforated cylindrical tubes located in the center portion of the channel. Also, in this case stable separated regions filled with air were formed downstream of the tubes, and the length of these regions increased with increasing velocity.

Nine-Tube Mixer with Abrupt Contraction. The void-fraction distribution observed was found to closely resemble that noted for the straight channel, except that the air was more-evenly distributed

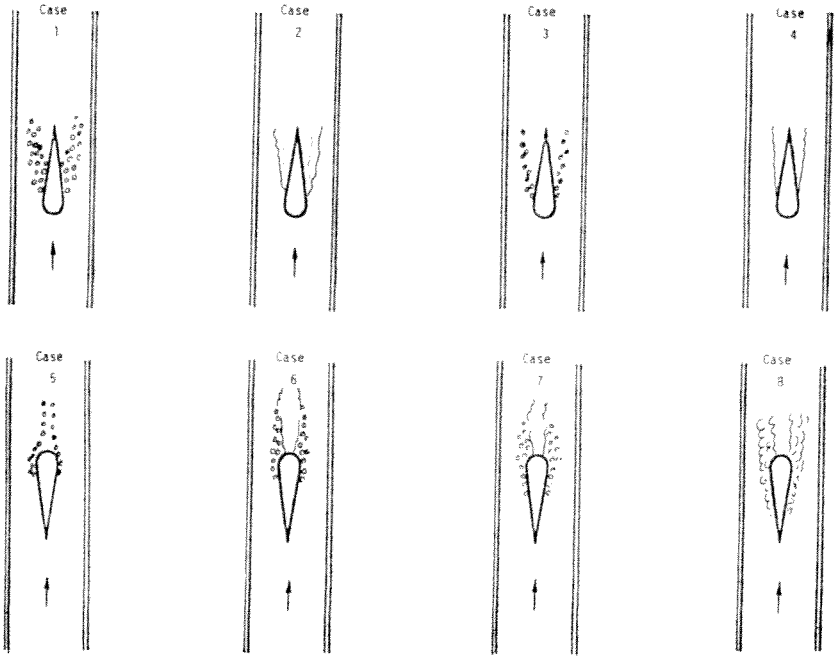

Fig. 13 Airfoil-shaped element in upward flow (Case 1 (low water and air flow): bubbles (~3–5 mm dia) emanate from trailing holes. Case 2 (low water and high air flow): a slug is generated at the surface (resembling film boiling) with a very turbulent interface. Case 3 (high water and low air flow): bubbles (~1 mm dia) emanate from leading holes. Case 4 (high water and medium air flow): separation occurs with a finely structured smooth interface. Case 5 (low water and air flow): bubbles (~3 mm dia) emanate from trailing holes with no separation. Case 6 (low water and medium air flow): bubbles (~3–5 mm dia) emanate and mix with separated region. Case 7 (medium water and low air flow): pattern similar to Case 6 but bubbles ~1–3 mm dia. Case 8 (low or medium water and high air flow): structure resembles film boiling with a very turbulent interface.) Flow rates at ambient pressure and temperature—Air: low: up to 0.0007 m^3/s, medium: from 0.0007 to 0.0018 m^3/s, high: above 0.0018 m^3/s. Water: low: up to 0.002 m^3/s, medium: from 0.002 to 0.007 m^3/s, high: above 0.007 m^3/s

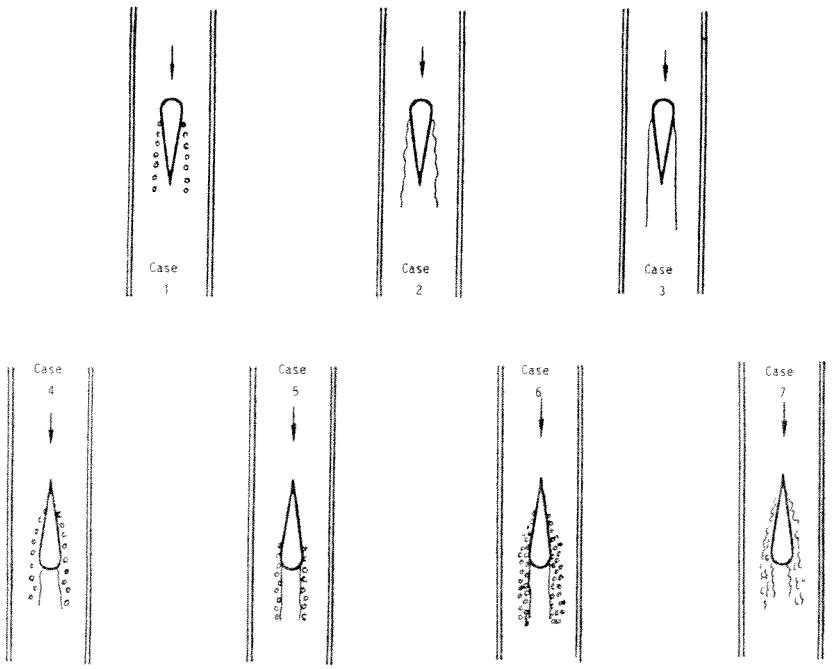

Fig. 14 Airfoil-shaped element in downward flow (Case 1 (low water and air flow): bubbles (~3–4 mm dia) emanate from leading holes only. Case 2 (low water and medium air flow): separation occurs with relatively smooth interface. Case 3 (medium or high water and low air flow): separation occurs with straight and smooth interface. Case 4 (low water and air flow): bubbles (~3–5 mm dia) emanate from leading holes only and then coalesce with separated region. Case 5 (high water and low air flow): bubbles (~1 mm dia) emanate from trailing holes and then coalesce with separated region. Case 6 (high water and medium air flow): bubbles (~1 mm dia) emanate from most of the holes and some coalesce with separated region. Case 7 (medium or high water and high air flow): structure resembles film boiling with a very turbulent interface and turbulent separated region.) Flow rates at ambient pressure and temperature—Air: low: up to 0.0007 m^3/s, medium: from 0.0007 to 0.0018 m^3/s, high: above 0.0018 m^3/s. Water: low: up to 0.002 m^3/s, medium: from 0.002 to 0.007 m^3/s, high: above 0.007 m^3/s

across the wide cross-sectional area (see Fig. 12). This was attributed to the forced turbulent mixing caused by the abrupt contraction. This was especially true at high water flow rates.

When the soap solution was injected for this configuration, a number of very small bubbles produced by the two-phase turbulence were observed. However, measurements displayed no appreciable change in void fraction distributions and only a slight increase in bubbling frequencies.

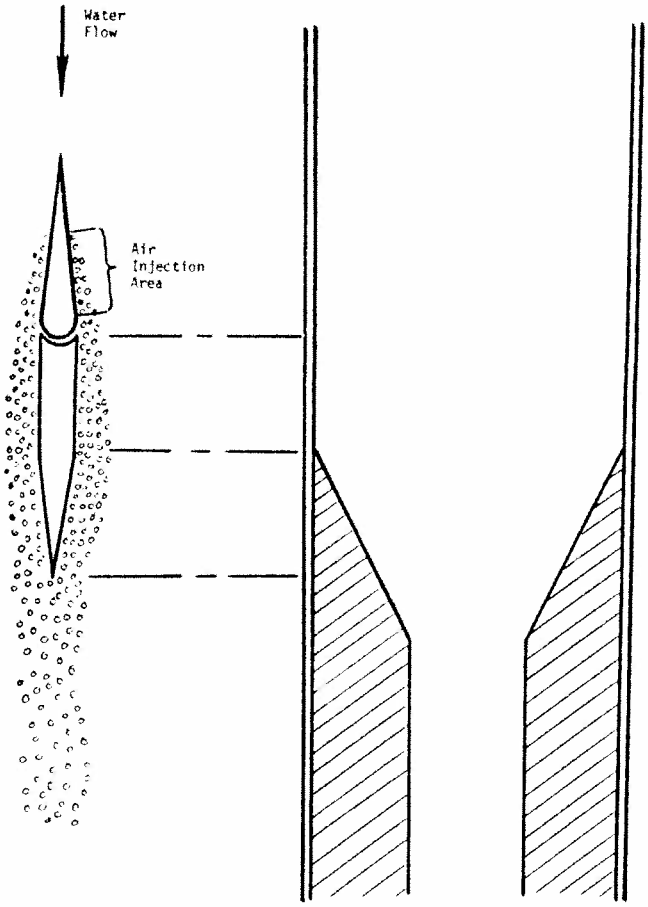

Fig. 15 Extended perforated-plate airfoil element with contraction

Perforated-Plate Airfoil Mixer. In addition to the above element tests, a series of semi-quantitative tests were run to initially investigate the flow structure produced by an airfoil-shaped mixer element. In this case two 3.8 cm-thick plexiglas plates were inserted, reducing the cross-sectional area to 4 × 1 in. (10 × 2.5 cm), as indicated by the dashed lines in Fig. 4. The element was installed in the center of this reduced channel and constructed from a perforated aluminum plate with 0.05-in. (0.13-cm) dia holes, constituting 23 percent open-surface area. The element is 3 in. (7.62 cm) long and 0.63 in. (1.6 cm) thick. Figs. 13 and 14 contain summary sketches of the flow regimes for various flow configurations. It was readily demonstrated from these experiments that the geometry of the mixer and the local pressure distribution decisively influenced the structure of the generated two-phase flow. The results from the various configurations are briefly summarized as follows:

Configuration 1 (upward flow with aligned element, Cases 1–4, Fig. 13). The lowest pressure region in the water flow adjacent to the mixer element was found to occur at the downstream holes of the element where the first air bubbles appeared. For high water velocities this region moved to the chord of the element. However, for high air injection rates the water flow was found to separate from the entire element area.

Configuration 2 (upward flow with reversed element, Cases 5–8, Fig. 13). As the water velocity increased along the element, resulting in a negative pressure gradient along the flow, the ejected bubbles were driven along the flow, and this tended to minimize their coalescence and postpone separation. Still, a separated region downstream of the bluff trailing edge formed. With high air flow, separation characterized by a very turbulent interface occurred at the element.

Configuration 3 (downward flow with aligned element, Cases 1–3, Fig. 14). Here the hydrostatic weight of the water increased the pressure gradient along the mixer element and this was found to enhance the onset of the type of flow separation observed for Configuration 1.

Configuration 4 (downward flow with reverse element, Cases 4–7, Fig. 14). In this configuration the type of separation analogous to that found for Configuration 2 was observed.

Based on these results another series of element tests were conducted to eliminate the separated region that occurred downstream of the bluff trailing edge for Configuration 3. The basic design of the

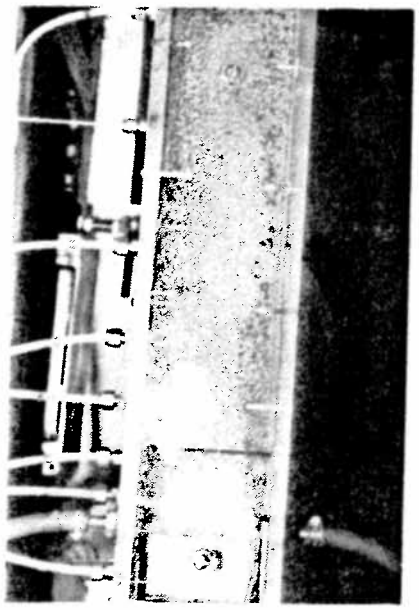

Fig. 16 Two-phase flow pattern obtained in tap water for a single porous airfoil mixer in a straight channel: low water and medium air flow rates

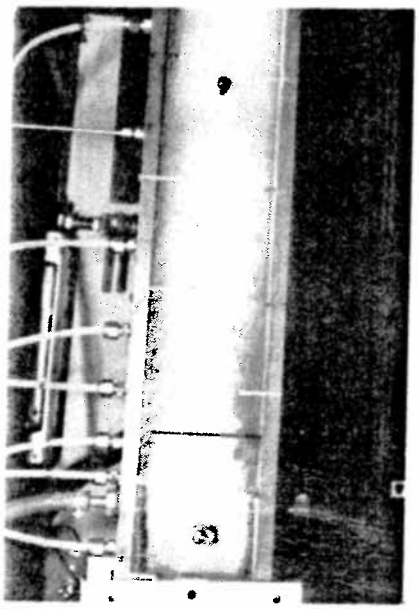

Fig. 17 Two-phase flow pattern obtained in soap-water solution for a single porous airfoil mixer in a straight channel: low water and medium air flow rates

extended element for these tests (Fig. 15) consisted of a gradually-tapered trailing edge with the surrounding channel walls contracting perpendicular to the tapered edge, but at a larger angle. This constriction forced the velocity to increase and the pressure to decrease along the flow, thereby eliminating flow separation at the trailing edge over a very wide range of gas injection rates.

Porous Airfoil Mixer. It was noticed in a number of the experiments with the perforated-plate mixer element that air was exiting from only two or three adjacent rows of holes. This occurred where the pressure in the water (or two-phase flow) was the lowest, since gas will exit where the highest positive pressure differential is available. To insure the generation of bubbles over the whole element, it is necessary to increase the pressure difference across the injection plate so that it exceeded the pressure difference in the water channel along the length of the element. For this reason, it was decided to make an airfoil shaped mixer element out of sintered porous metal with 10 μm dia pores. The element was placed with the narrower edge facing a flow that was vertically upwards. The air and water flow patterns for low flow rates are given in Fig. 16. Bubbles about 3 mm in diameter were obtained. Higher water velocities yielded smaller bubbles while higher air flow rates eventually caused transition to slug flow and hydrodynamic instability.

The effect of the addition of a surfactant (soap solution) is illustrated in Fig. 17. The air and water flow rates are the same as for Fig. 16. It is striking to see that the diameter of the bubbles was decreased by a factor of five to ten, hence their volume decreased by a factor of a hundred to a thousand. The relative slip velocity (or rise velocity) of these tiny bubbles appeared to be lower. (This can easily be observed when bubbling through stagnant water.) When the air injection rate was high, the two-phase flow at the element resembled that found in film boiling. Large gas slugs were present in the downstream flow, but they were more difficult to observe due to presence of many tiny bubbles with the soap surfactant.

Conclusions and Summary

Results from these experiments indicate that element and contraction-geometry designs are the most critical factors in mixer development. Two-phase flow turbulence is not effective itself in the creation of a homogeneous two-phase flow at high void fractions even in strongly surface-active systems. This is somewhat contrary to the behavior at low void fractions where turbulence breaks large bubbles into smaller ones. It seems that in some mixers churn turbulent slug flow is established in the mixer and is maintained further downstream regardless of the level of surface activity of the system. (One explanation of how agitation may act to destroy foam is given by Prins [9].)

A favorable (decreasing) pressure gradient in and downstream from the injection region tends to drive bubbles along the flow and postpone their possible coalescence and hence the creation of separated regions. The latter themselves could be sources of large bubbles or slugs. The most effective way of insuring the existence of a favorable pressure gradient was found in the experiments to be through the use of various contraction geometries. Such contractions can have other beneficial effects, such as decreased frictional and two-phase mixing losses upstream of an LMMHD generator. Further, since high velocities are desired in LMMHD generators (perhaps as high as 50 m/s), high pressure drops across the contraction will exist. This is advantageous since the actual two-phase mixing is accomplished at higher pressures and lower void fractions where it is easier to create a homogeneous bubbly flow. Expansion of the bubbly flow through the contraction represents a favorable condition for the stabilization of the foam flow since no additional flow disturbances are introduced, and leads to the higher void fractions desired at the generator entrance.

The literature and the above experiments show that the injection of gas through porous surfaces should be done at low superficial velocities (volumetric gas flow rate/total porous area), i.e., below the critical velocity at which hydrodynamic instability creates gas slugs at the injection surface. A low injection velocity, however, requires a relatively-large injection surface, which can be best achieved through the use of several long airfoil-shaped elements.

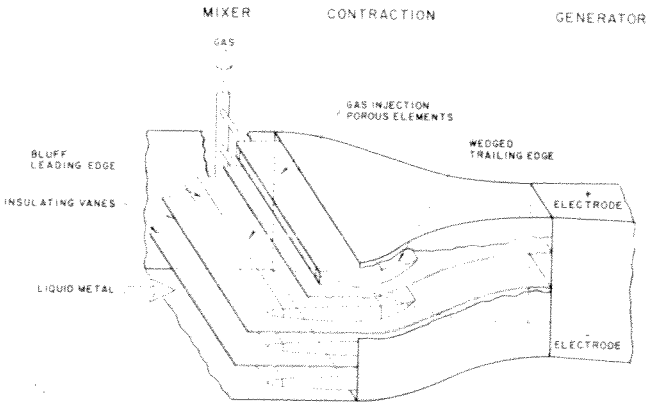

Fig. 18 Conceptual design of mixer-generator inlet assembly

The findings of this research have led to the conceptual design of a two-phase LMMHD mixer shown in Fig. 18. By placing a contraction and several long porous mixer elements upstream of the generator, a large-enough area is provided for the injection of the gas, thus ensuring a below-critical injection velocity and the creation of a multitude of small bubbles. The wedged-element trailing edges are placed in the two-dimensional contraction to provide for smooth transition in the flow, thereby preventing separation. (In this design, a continuous-accelerating region actually exists all the way from the leading edge of the porous elements to the beginning of the LMMHD generator.) The resulting favorable pressure gradient ensures that the wall boundary layers are thin and laminar. In this way, losses in the mixer are minimized.

Acknowledgment

The authors wish to acknowledge Dr. E. S. Pierson for his comments and support during the course of this research, and Mr. Robert Kolp for his technical assistance.

References

1 Fabris, G., and Hantman, R. G., "Fluid Dynamic Aspects of Liquid-Metal Gas Two-Phase Magnetohydrodynamic Power Generators," *Proceedings of the 1976 Heat Transfer and Fluid Mechanics Institute*, Davis, CA, Stanford University Press, 1976, pp. 92–113.

2 Fabris, G., Cole, R., and Hantman, R. G., "Fluid Dynamic Studies of Two-Phase Liquid Metal Flow in an MHD Generator," *Proceedings of the 6th International Conference on MHD Electrical Power Generation*, Vol. 3, Washington, D. C., 1975, pp. 363–376.

3 Kling, G., "Über die Dynamik der Blasenbildung beim Begasen von Flüssigkeiten unter Druck," *International Journal of Heat and Mass Transfer*, Vol. 5, 1962, pp. 211–223.

4 Wallis, G. B., "Some Hydrodynamic Aspects of Two-Phase Flow and Boiling," *International Development in Heat Transfer*, ASME Paper 38, Vol. 2, 1961, pp. 319–340.

5 Staub, F. W., "Flow Regimes and Mixture Densities in Froth-Foam Columns," *Proceedings of the Meeting of American Institute of Chemical Engineers*, Boston, Sept. 1975.

6 Fujii-e, Y., Miyazaki, K., Inoue, S., Saito, M., and Suita, F., "Experimental Study on Two-Phase Induction Power Generation using NaK-N_2 Mixture," *Proceedings of the 6th International Conference on MHD Electrical Power Generation*, Vol. 3, Washington, D. C., 1975, pp. 247–263.

7 Prins, A., "Dynamic Surface Properties and Foaming Behavior of Aqueous Surfactant Solutions," *Foams*, R. J. Akers, ed., Pergamon Press, 1976, pp. 51–60.

8 Adler, P. M., "Formation of an Air-Water Two-Phase Flow," *AIChE Journal*, Vol. 23, 1977, pp. 185–191.